Fermi National Accelerator Laboratory

D0 Results on W Boson Properties

B. Abbott et al.

The D0 Collaboration

Fermi National Accelerator Laboratory
P.O. Box 500, Batavia, Illinois 60510

October 1997

Disclaimer

DØ Results on W Boson Properties

The DØ Collaboration *
Fermi National Accelerator Laboratory, Batavia, Illinois 60510
(July 1, 1997)

Abstract

The DØ experiment collected $\approx$ 15 pb^{-1} in run 1A (1992-1993) and $\approx$ 89 pb^{-1} in run 1B (1994-1995) of the Fermilab Tevatron Collider using $p\bar{p}$ collisions at $\sqrt{s}$ = 1.8 TeV. Results from analyses of events with W and Z bosons are presented for the run 1B data samples. From $W \rightarrow e\nu, \mu\nu$ and $Z \rightarrow ee, \mu\mu$ decays, the W and Z production cross sections and the W width are determined. Events with $W \rightarrow \tau\nu$ decays are used to determine the ratio of the electroweak gauge coupling constants as a measure of lepton universality. Using $W \rightarrow e\nu$ and $Z \rightarrow ee$ decays, the W boson mass is measured.

B. Abbott,[28] M. Abolins,[25] B.S. Acharya,[43] I. Adam,[12] D.L. Adams,[37] M. Adams,[17]
S. Ahn,[14] H. Aihara,[22] G.A. Alves,[10] E. Amidi,[29] N. Amos,[24] E.W. Anderson,[19] R. Astur,[42]
M.M. Baarmand,[42] A. Baden,[23] V. Balamurali,[32] J. Balderston,[16] B. Baldin,[14]
S. Banerjee,[43] J. Bantly,[5] J.F. Bartlett,[14] K. Bazizi,[39] A. Belyaev,[26] S.B. Beri,[34]
I. Bertram,[31] V.A. Bezzubov,[35] P.C. Bhat,[14] V. Bhatnagar,[34] M. Bhattacharjee,[13]
N. Biswas,[32] G. Blazey,[30] S. Blessing,[15] P. Bloom,[7] A. Boehnlein,[14] N.I. Bojko,[35]
F. Borcherding,[14] C. Boswell,[9] A. Brandt,[14] R. Brock,[25] A. Bross,[14] D. Buchholz,[31]
V.S. Burtovoi,[35] J.M. Butler,[3] W. Carvalho,[10] D. Casey,[39] Z. Casilum,[42]
H. Castilla-Valdez,[11] D. Chakraborty,[42] S.-M. Chang,[29] S.V. Chekulaev,[35] L.-P. Chen,[22]
W. Chen,[42] S. Choi,[41] S. Chopra,[24] B.C. Choudhary,[9] J.H. Christenson,[14] M. Chung,[17]
D. Claes,[27] A.R. Clark,[22] W.G. Cobau,[23] J. Cochran,[9] W.E. Cooper,[14] C. Cretsinger,[39]
D. Cullen-Vidal,[5] M.A.C. Cummings,[16] D. Cutts,[5] O.I. Dahl,[22] K. Davis,[2] K. De,[44]
K. Del Signore,[24] M. Demarteau,[14] D. Denisov,[14] S.P. Denisov,[35] H.T. Diehl,[14]
M. Diesburg,[14] G. Di Loreto,[25] P. Draper,[44] Y. Ducros,[40] L.V. Dudko,[26] S.R. Dugad,[43]
D. Edmunds,[25] J. Ellison,[9] V.D. Elvira,[42] R. Engelmann,[42] S. Eno,[23] G. Eppley,[37]
P. Ermolov,[26] O.V. Eroshin,[35] V.N. Evdokimov,[35] T. Fahland,[8] M. Fatyga,[4] M.K. Fatyga,[39]
J. Featherly,[4] S. Feher,[14] D. Fein,[2] T. Ferbel,[39] G. Finocchiaro,[42] H.E. Fisk,[14] Y. Fisyak,[7]
E. Flattum,[14] G.E. Forden,[2] M. Fortner,[30] K.C. Frame,[25] S. Fuess,[14] E. Gallas,[44]
A.N. Galyaev,[35] P. Gartung,[9] T.L. Geld,[25] R.J. Genik II,[25] K. Genser,[14] C.E. Gerber,[14]
B. Gibbard,[4] S. Glenn,[7] B. Gobbi,[31] M. Goforth,[15] A. Goldschmidt,[22] B. Gómez,[1]
G. Gómez,[23] P.I. Goncharov,[35] J.L. González Solís,[11] H. Gordon,[4] L.T. Goss,[45]
K. Gounder,[9] A. Goussiou,[42] N. Graf,[4] P.D. Grannis,[42] D.R. Green,[14] J. Green,[30]
H. Greenlee,[14] G. Grim,[7] S. Grinstein,[6] N. Grossman,[14] P. Grudberg,[22] S. Grünendahl,[39]
G. Guglielmo,[33] J.A. Guida,[2] J.M. Guida,[5] A. Gupta,[43] S.N. Gurzhiev,[35] P. Gutierrez,[33]
Y.E. Gutnikov,[35] N.J. Hadley,[23] H. Haggerty,[14] S. Hagopian,[15] V. Hagopian,[15]
K.S. Hahn,[39] R.E. Hall,[8] P. Hanlet,[29] S. Hansen,[14] J.M. Hauptman,[19] D. Hedin,[30]
A.P. Heinson,[9] U. Heintz,[14] R. Hernández-Montoya,[11] T. Heuring,[15] R. Hirosky,[15]
J.D. Hobbs,[14] B. Hoeneisen,[1,†] J.S. Hoftun,[5] F. Hsieh,[24] Ting Hu,[42] Tong Hu,[18] T. Huehn,[9]
A.S. Ito,[14] E. James,[2] J. Jaques,[32] S.A. Jerger,[25] R. Jesik,[18] J.Z.-Y. Jiang,[42]
T. Joffe-Minor,[31] K. Johns,[2] M. Johnson,[14] A. Jonckheere,[14] M. Jones,[16] H. Jöstlein,[14]
S.Y. Jun,[31] C.K. Jung,[42] S. Kahn,[4] G. Kalbfleisch,[33] J.S. Kang,[20] R. Kehoe,[32] M.L. Kelly,[32]
C.L. Kim,[20] S.K. Kim,[41] A. Klatchko,[15] B. Klima,[14] C. Klopfenstein,[7] V.I. Klyukhin,[35]
V.I. Kochetkov,[35] J.M. Kohli,[34] D. Koltick,[36] A.V. Kostritskiy,[35] J. Kotcher,[4]
A.V. Kotwal,[12] J. Kourlas,[28] A.V. Kozelov,[35] E.A. Kozlovski,[35] J. Krane,[27]
M.R. Krishnaswamy,[43] S. Krzywdzinski,[14] S. Kunori,[23] S. Lami,[42] H. Lan,[14,*] R. Lander,[7]
F. Landry,[25] G. Landsberg,[14] B. Lauer,[19] A. Leflat,[26] H. Li,[42] J. Li,[44] Q.Z. Li-Demarteau,[14]
J.G.R. Lima,[38] D. Lincoln,[24] S.L. Linn,[15] J. Linnemann,[25] R. Lipton,[14] Q. Liu,[14,*]
Y.C. Liu,[31] F. Lobkowicz,[39] S.C. Loken,[22] S. Lökös,[42] L. Lueking,[14] A.L. Lyon,[23]
A.K.A. Maciel,[10] R.J. Madaras,[22] R. Madden,[15] L. Magaña-Mendoza,[11] S. Mani,[7]
H.S. Mao,[14,*] R. Markeloff,[30] T. Marshall,[18] M.I. Martin,[14] K.M. Mauritz,[19] B. May,[31]
A.A. Mayorov,[35] R. McCarthy,[42] J. McDonald,[15] T. McKibben,[17] J. McKinley,[25]
T. McMahon,[33] H.L. Melanson,[14] M. Merkin,[26] K.W. Merritt,[14] H. Miettinen,[37]
A. Mincer,[28] C.S. Mishra,[14] N. Mokhov,[14] N.K. Mondal,[43] H.E. Montgomery,[14]
P. Mooney,[1] H. da Motta,[10] C. Murphy,[17] F. Nang,[2] M. Narain,[14] V.S. Narasimham,[43]
A. Narayanan,[2] H.A. Neal,[24] J.P. Negret,[1] P. Nemethy,[28] M. Nicola,[10] D. Norman,[45]

L. Oesch,[24] V. Oguri,[38] E. Oltman,[22] N. Oshima,[14] D. Owen,[25] P. Padley,[37] M. Pang,[19]
A. Para,[14] Y.M. Park,[21] R. Partridge,[5] N. Parua,[43] M. Paterno,[39] J. Perkins,[44] M. Peters,[16]
R. Piegaia,[6] H. Piekarz,[15] Y. Pischalnikov,[36] V.M. Podstavkov,[35] B.G. Pope,[25]
H.B. Prosper,[15] S. Protopopescu,[4] J. Qian,[24] P.Z. Quintas,[14] R. Raja,[14] S. Rajagopalan,[4]
O. Ramirez,[17] L. Rasmussen,[42] S. Reucroft,[29] M. Rijssenbeek,[42] T. Rockwell,[25] N.A. Roe,[22]
P. Rubinov,[31] R. Ruchti,[32] J. Rutherfoord,[2] A. Sánchez-Hernández,[11] A. Santoro,[10]
L. Sawyer,[44] R.D. Schamberger,[42] H. Schellman,[31] J. Sculli,[28] E. Shabalina,[26] C. Shaffer,[15]
H.C. Shankar,[43] R.K. Shivpuri,[13] M. Shupe,[2] H. Singh,[9] J.B. Singh,[34] V. Sirotenko,[30]
W. Smart,[14] R.P. Smith,[14] R. Snihur,[31] G.R. Snow,[27] J. Snow,[33] S. Snyder,[4] J. Solomon,[17]
P.M. Sood,[34] M. Sosebee,[44] N. Sotnikova,[26] M. Souza,[10] A.L. Spadafora,[22]
R.W. Stephens,[44] M.L. Stevenson,[22] D. Stewart,[24] F. Stichelbaut,[42] D.A. Stoianova,[35]
D. Stoker,[8] M. Strauss,[33] K. Streets,[28] M. Strovink,[22] A. Sznajder,[10] P. Tamburello,[23]
J. Tarazi,[8] M. Tartaglia,[14] T.L.T. Thomas,[31] J. Thompson,[23] T.G. Trippe,[22] P.M. Tuts,[12]
N. Varelas,[25] E.W. Varnes,[22] D. Vititoe,[2] A.A. Volkov,[35] A.P. Vorobiev,[35] H.D. Wahl,[15]
G. Wang,[15] J. Warchol,[32] G. Watts,[5] M. Wayne,[32] H. Weerts,[25] A. White,[44] J.T. White,[45]
J.A. Wightman,[19] S. Willis,[30] S.J. Wimpenny,[9] J.V.D. Wirjawan,[45] J. Womersley,[14]
E. Won,[39] D.R. Wood,[29] H. Xu,[5] R. Yamada,[14] P. Yamin,[4] C. Yanagisawa,[42] J. Yang,[28]
T. Yasuda,[29] P. Yepes,[37] C. Yoshikawa,[16] S. Youssef,[15] J. Yu,[14] Y. Yu,[41] Z.H. Zhu,[39]
D. Zieminska,[18] A. Zieminski,[18] E.G. Zverev,[26] and A. Zylberstejn[40]

(DØ Collaboration)

[1]Universidad de los Andes, Bogotá, Colombia
[2]University of Arizona, Tucson, Arizona 85721
[3]Boston University, Boston, Massachusetts 02215
[4]Brookhaven National Laboratory, Upton, New York 11973
[5]Brown University, Providence, Rhode Island 02912
[6]Universidad de Buenos Aires, Buenos Aires, Argentina
[7]University of California, Davis, California 95616
[8]University of California, Irvine, California 92697
[9]University of California, Riverside, California 92521
[10]LAFEX, Centro Brasileiro de Pesquisas Físicas, Rio de Janeiro, Brazil
[11]CINVESTAV, Mexico City, Mexico
[12]Columbia University, New York, New York 10027
[13]Delhi University, Delhi, India 110007
[14]Fermi National Accelerator Laboratory, Batavia, Illinois 60510
[15]Florida State University, Tallahassee, Florida 32306
[16]University of Hawaii, Honolulu, Hawaii 96822
[17]University of Illinois at Chicago, Chicago, Illinois 60607
[18]Indiana University, Bloomington, Indiana 47405
[19]Iowa State University, Ames, Iowa 50011
[20]Korea University, Seoul, Korea
[21]Kyungsung University, Pusan, Korea
[22]Lawrence Berkeley National Laboratory and University of California, Berkeley, California 94720
[23]University of Maryland, College Park, Maryland 20742
[24]University of Michigan, Ann Arbor, Michigan 48109
[25]Michigan State University, East Lansing, Michigan 48824
[26]Moscow State University, Moscow, Russia
[27]University of Nebraska, Lincoln, Nebraska 68588
[28]New York University, New York, New York 10003
[29]Northeastern University, Boston, Massachusetts 02115
[30]Northern Illinois University, DeKalb, Illinois 60115
[31]Northwestern University, Evanston, Illinois 60208
[32]University of Notre Dame, Notre Dame, Indiana 46556
[33]University of Oklahoma, Norman, Oklahoma 73019
[34]University of Panjab, Chandigarh 16-00-14, India
[35]Institute for High Energy Physics, 142-284 Protvino, Russia
[36]Purdue University, West Lafayette, Indiana 47907
[37]Rice University, Houston, Texas 77005
[38]Universidade do Estado do Rio de Janeiro, Brazil
[39]University of Rochester, Rochester, New York 14627
[40]CEA, DAPNIA/Service de Physique des Particules, CE-SACLAY, Gif-sur-Yvette, France
[41]Seoul National University, Seoul, Korea
[42]State University of New York, Stony Brook, New York 11794
[43]Tata Institute of Fundamental Research, Colaba, Mumbai 400005, India
[44]University of Texas, Arlington, Texas 76019
[45]Texas A&M University, College Station, Texas 77843

4

I. INTRODUCTION

The DØ experiment collected ≈ 15 pb^{-1} in run 1A (1992-1993) and ≈ 89 pb^{-1} in run 1B (1994-1995) of the Fermilab Tevatron Collider using $p\bar{p}$ collisions at $\sqrt{s} = 1.8$ TeV. Results are presented from data collected by the DØ experiment that test the Standard Model (SM) of electroweak interactions [1]. Measurements of the W and Z boson production cross sections, the W decay width, the ratio of the gauge coupling constants, and the W mass are presented.

II. THE DØ DETECTOR

The DØ detector was designed to study a variety of high transverse momentum (p_T) physics topics and has been described in detail elsewhere [2]. It does not have a central magnetic field, making possible a compact, hermetic detector with almost full solid angle coverage. The detector has an inner tracking system which measures charged tracks to a pseudo-rapidity $\eta < 3.2$, where $\eta = -\ln \tan \frac{\theta}{2}$ and θ is the polar angle. The tracking system is surrounded by finely-segmented uranium liquid-argon calorimeters (one central and two end-caps). Surrounding the calorimeter is a muon magnetic spectrometer which consists of magnetized iron toroids that are situated between the first two of three layers of proportional drift tubes.

Electrons and photons were identified by the shape of their energy deposition in the calorimeter and a matching track (for electrons). The energy (E) was measured by the calorimeter with a resolution of $\approx 15\%/\sqrt{E}$ (GeV). Neutrinos were not identified in the detector but their transverse momentum was inferred from the missing transverse energy in the event: $\vec{\not{E}}_T = -\sum_i E_i \sin \theta$, where the sum i extends over all cells in the calorimeter. Muons were identified by a track in the muon chambers matched with a track in the central tracking chambers.

III. W AND Z PRODUCTION

Events in which a W or Z boson is produced are used to measure the cross section times branching fraction, the W width and the ratio of the gauge couplings. In these analyses, the W and Z gauge bosons are identified through their leptonic decay modes: $W \rightarrow e\nu, \mu\nu, \tau\nu$ and $Z \rightarrow ee, \mu\mu$. These modes have a cleaner signature and are easier to distinguish from the background of QCD multijet production than hadronic decay modes. The events with decays into e's and μ's are selected by requiring a high-p_T e or μ and large $\not{E}_T$ for W's and two high-p_T e's or μ's for Z's. The hadronic decay of the τ is used to to select the $W \rightarrow \tau\nu$ events.

A. Production Cross Sections

The measurement of the product of the cross section and the branching fraction for W's and Z's provides a fundamental test of the Standard Model. These measurements have been

published for the run 1A data sample [3] and the preliminary results are presented here for the run 1B data sample.

For the final event selection in this analysis, electrons were restricted to a region $|\eta| < 1.1$ and $1.5 < |\eta| < 2.5$ and muons to a region $|\eta| < 1.0$. The $W \to e\nu$ events were selected by requiring the transverse energy of the electron $E_T > 25$ GeV and $\not{E}_T > 25$ GeV and the $Z \to ee$ events were required to have two e's with $E_T > 25$ GeV. The $W \to \mu\nu$ event selection required $p_T(\mu) > 20$ GeV, and $\not{E}_T > 20$ GeV and the $Z \to \mu\mu$ selection required $p_T > 15, 20$ GeV for the two μ's. The transverse mass for W events and invariant mass for Z events in the final data samples are shown in Fig. 1. Table I gives the number of events observed, the acceptance, the efficiency, the background and the luminosity for these data samples.
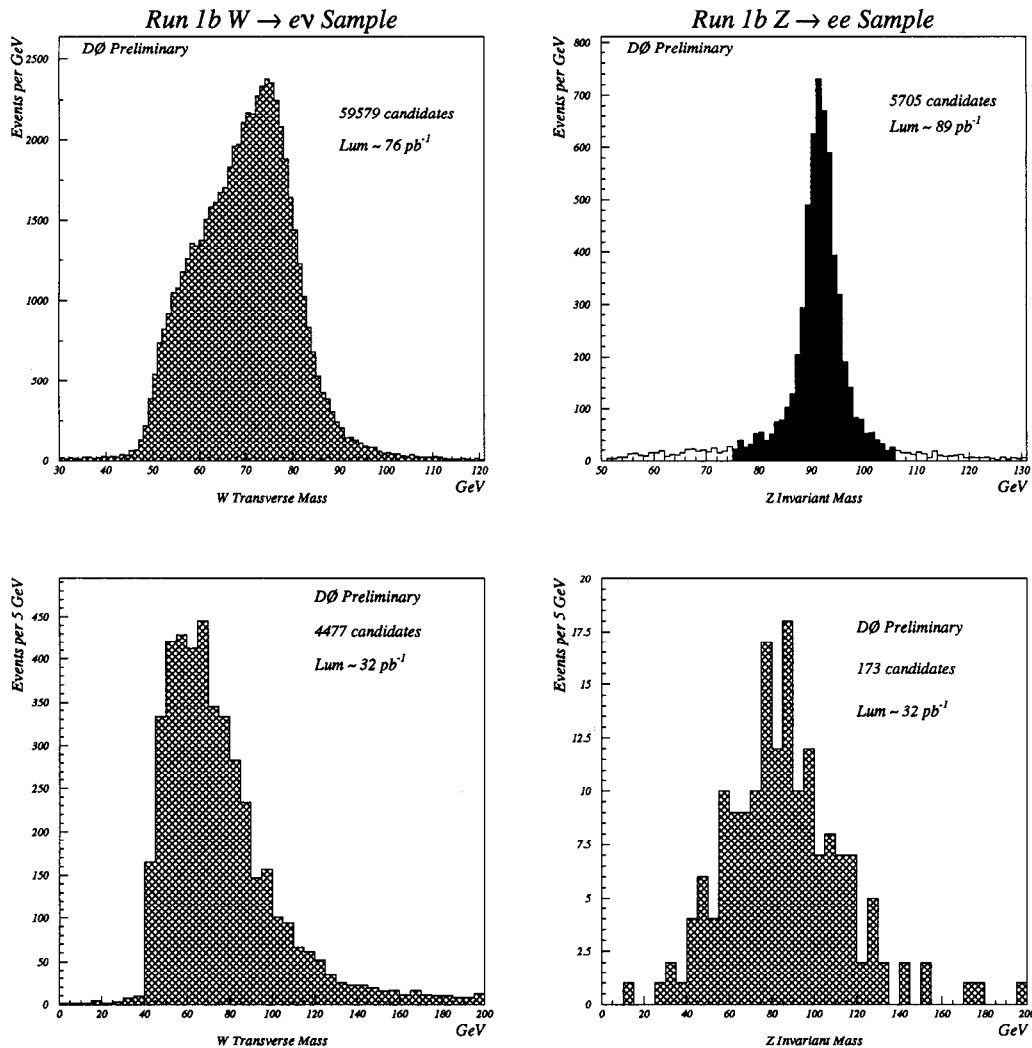
FIG. 1. Transverse and invariant mass distributions for the $W \to e\nu, \mu\nu$ and $Z \to ee, \mu\mu$ run 1B data samples.

6

	Electron	Muon
# W candidates	59579	4472
Acceptance (%)	43.4 ± 1.5	20.1 ± 0.7
ϵ_W (%)	70.0 ± 1.2	24.7 ± 1.5
Background(%)	8.1 ± 0.9	18.6 ± 2.0
Luminosity (pb^{-1})	75.9 ± 6.4	32.0 ± 2.7
# Z candidates	5702	173
A_Z(%)	34.2 ± 0.5	5.7 ± 0.5
ϵ_Z(%)	75.9 ± 1.2	43.2 ± 3.0
Bkg.(%)	4.8 ± 0.5	8.0 ± 2.1
Lum. (pb^{-1})	89.1 ± 7.5	32.0 ± 2.7

TABLE I. The quantities used to measure the preliminary cross sections for $W \to e\nu, \mu\nu$ and $Z \to ee, \mu\mu$ for the run 1B data sample.

The preliminary measurements of the cross section times branching fraction $(\sigma \cdot B)$ are given in table II and are shown in Fig. 2 along with the results from CDF [4]. The τ results shown will be discussed in section III C. Also shown in Fig. 2 are comparisons of $\sigma \cdot B$ with SM predictions [5]. The predictions use the CTEQ2M parton distribution functions (pdf) [6].
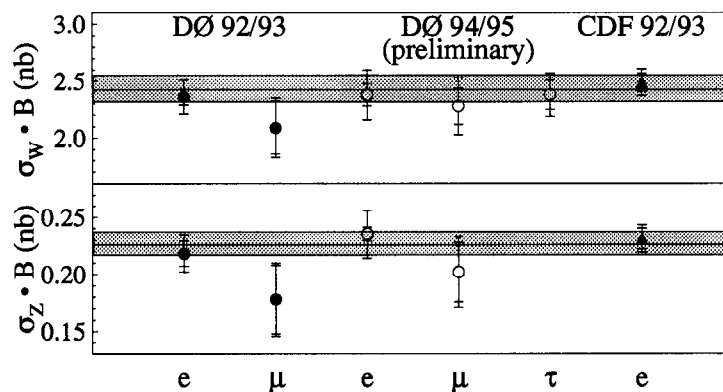
FIG. 2. Tevatron measurements for the cross sections times branching ratios for $W \to e\nu, \mu\nu, \tau\nu$ and $Z \to ee, \mu\mu$ compared to SM predictions.

B. W width

The ratio of the W and Z production cross sections can be used to measure the leptonic branching ratio $B(W \to l\nu)$ and extract the W width (Γ_W). From the measured width,

$\sigma_W \cdot B(W \to e\nu)$	=	2.38	$\pm\, 0.01$	$\pm\, 0.09$	$\pm\, 0.20$ nb
$\sigma_W \cdot B(W \to \mu\nu)$	=	2.32	$\pm\, 0.04$	$\pm\, 0.16$	$\pm\, 0.19$ nb
$\sigma_Z \cdot B(Z \to ee)$	=	0.235	$\pm\, 0.003$	$\pm\, 0.005$	$\pm\, 0.020$ nb
$\sigma_Z \cdot B(Z \to \mu\mu)$	=	0.202	$\pm\, 0.016$	$\pm\, 0.020$	$\pm\, 0.017$ nb
			$(\pm$stat$)$	$(\pm$syst$)$	$(\pm$lum$)$

TABLE II. The preliminary cross sections for $W \to e\nu, \mu\nu$ and $Z \to ee, \mu\mu$.

a limit may be placed on unexpected decay modes of the W. Many common systematic errors, including the luminosity error, cancel in the leptonic branching ratio:

$$R = \frac{\sigma_W \cdot B(W \to l\nu)}{\sigma_Z \cdot B(Z \to ll)} = \frac{\sigma_W}{\sigma_Z} \frac{\Gamma(W \to l\nu)}{\Gamma(Z \to ll)} \frac{\Gamma_Z}{\Gamma_W}.$$

Using the results above for $\sigma \cdot B$ and combining the electron and muon measurements, we obtain a preliminary run 1B result of $R = 10.32 \pm 0.43$. The leptonic branching fraction of the W may then be calculated, $B(W \to l\nu) = B(Z \to ll) \cdot (\sigma_Z/\sigma_W) \cdot R = (10.43 \pm 0.44)\%$ using the measured value of R, the value of $B(Z \to ll)$ from LEP measurements [7] and $\sigma_W/\sigma_Z = 3.33 \pm 0.03$ from the SM prediction [8]. The total width of the W is then obtained from this measurement of $B(W \to l\nu)$ and the value of $\Gamma(W \to l\nu)$ from SM predictions [9]. The preliminary run 1B measurement is

$$\Gamma_W = 2.159 \pm 0.092 \text{ GeV}.$$

Comparison of the published world average $\Gamma_W = 2.062 \pm 0.059$ GeV [3] (does not include the run 1B measurement) with the SM prediction $\Gamma_W = 2.077 \pm 0.014$ GeV [9], gives a 95% confidence level upper limit of $\Delta\Gamma_W < 109$ MeV on unexpected (non-SM) decays of the W.

C. Measurement of the Ratio of the Couplings

The decay $W \to \tau\nu$ is studied as a test of lepton universality by measuring the ratio of the electroweak coupling constants g_τ^W/g_e^W. The τ events are obtained from a sample in which inelastic collisions were selected by requiring a single interaction signature from the Level 0 trigger. The integrated luminosity for the τ trigger used in this analysis is 16.8 ± 0.9 pb^{-1}.

To select the $W \to \tau\nu$ events from the W data sample, the hadronic decay of the τ is used. These events are identified by the presence of an isolated, narrow jet. Jets were reconstructed using a cone algorithm with radius 0.7 in $\eta - \phi$ space and the width of the jet was required to be $rms_{jet} < 0.25$. The requirements that E_T(jet)> 25 GeV, $(|\eta| < 0.9)$, $\not{E}_T > 25$ GeV and that there be no opposite jet were placed on the data sample. In order to separate the events with a jet from a τ decay from the large background of QCD jets, the profile distribution of the jets is used. The profile is defined as the sum of the highest two tower E_T's divided by the cluster E_T. The profile distributions from the τ sample and

the QCD background sample (selected from events with low $\not{E}_T$) are shown in Fig. 3. A requirement that the profile variable be > 0.55 is made to select the final τ event sample. The shaded low-profile region in Fig. 3a is used to estimate the remaining QCD background.
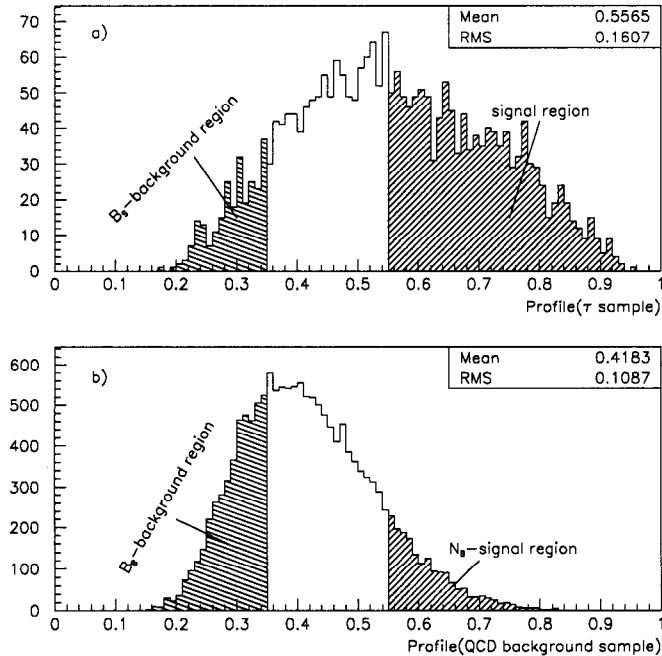
FIG. 3. The distribution of the profile quantity for the τ candidate sample and for the QCD background sample.

The number of signal events contained in the final data sample is listed in table III along with the estimated background contributions. The preliminary value of the cross section times branching ratio is $\sigma \cdot B(W \to \tau\nu) = 2.38 \pm 0.09(stat) \pm 0.10(syst)$ nb where the error due to the luminosity has not been included. Comparing this value with the measurement of $\sigma \cdot B(W \to e\nu)$ from run 1A [3], the ratio of the couplings is determined $g_\tau^W/g_e^W = 1.004 \pm 0.019(stat) \pm 0.026(syst)$. This measurement shows good agreement with $e - \tau$ universality at high energy.

IV. W MASS

The electroweak Standard Model can be specified by three parameters. These may be taken to be α, G_F and M_Z, all measured to $< 0.01\%$. At lowest order, the W mass is precisely defined as $M_W = A/\sin\theta_W$ with $\sin^2\theta_W = 1 - M_W^2/M_Z^2$, where θ_W is the weak mixing angle and $A = (\pi\alpha/\sqrt{2}G_F)^{1/2}$. The current data are sufficiently precise to require comparison to theoretical predictions which include higher order corrections. These corrections have contributions due to the running of $\alpha \to \alpha(M_Z^2)$ and to loop diagrams which introduce a

9

	Number of Events
Final Data Sample	1202
QCD Background	$106 \pm 7 \pm 5$
Noise Events	81 ± 14
$Z \to \tau\tau$	32 ± 5
$W \to e\nu$	3 ± 1

TABLE III. The quantities used to measure the run 1B preliminary cross section for $W \to \tau\nu$.

dependence on the square of the top quark mass, m_{top}, and the log of the Higgs mass, M_H. A precision measurement of the W mass therefore defines the size of the radiative corrections in the SM and along with m_{top} it can constrain M_H. A direct measurement also serves to test the consistency of the SM.

Previous results from the run 1A data sample have been published [10] and yielded a value of $M_W = 80.350 \pm 0.270$ GeV/c^2. In the analysis presented here, the preliminary measurement of M_W from the run 1B data sample is presented, using a calorimeter-based measurement. The calorimeter is not calibrated independently to the precision needed and therefore the ratio of the W to Z masses was measured and then scaled to the precisely known ($< 0.01\%$) Z mass [11]. Many systematic errors cancel in this ratio.

Experimentally, the remnants of the interaction $p\bar{p} \to W(\to e\nu) + X$ are detected. Here X is due to the recoil (rec) to the W plus the underlying event. The energy of the electron and the $\vec{\not{E}}_T$ were measured. The $\vec{\not{E}}_T = -\vec{p}_T(rec) - \vec{p}_T(e) = \vec{p}_T(W) - \vec{p}_T(e)$ and is identified with the neutrino transverse momentum $\vec{p}_T(\nu)$ but differs from $\vec{p}_T(\nu)$ because of the presence of the underlying event.

Because the longitudinal momentum of the ν is not measured, the W invariant mass cannot be constructed. Instead the distribution in transverse mass $M_T(W) = \sqrt{2p_T(e)p_T(\nu) - 2\vec{p}_T(e) \cdot \vec{p}_T(\nu)}$ is used to obtain the W mass. For Z decays, the energies of both electrons are measured and the invariant mass is reconstructed.

The $W \to e\nu$ events were selected by requiring an isolated electron with $E_T > 25$ GeV, $p_T(W) < 15$ GeV/c and $\not{E}_T > 25$ GeV. The $Z \to ee$ events were selected by requiring two isolated electrons each with $E_T > 25$ GeV, and $70 < M_Z < 110$ GeV/c^2. Electrons were required to be in the region $|\eta| < 1.0$. There were 28323 W events and 2179 Z events in this sample. The electron polar angle was determined from the shower centroid of the energy cluster in the electromagnetic (EM) calorimeter and the center-of-gravity of the corresponding track. The uncertainty in determining this angle results in an uncertainty of ± 28 MeV/c^2 in M_W.

The mass of the W is determined by a maximum likelihood fit of the measured $M_T(W)$ distribution to Monte Carlo (MC) distributions which were generated for 21 different values of M_W in 100 MeV steps. This fast MC simulation uses a theoretical calculation for the W production and decay and a parameterized model for the detector response. Kinematic cuts are placed on the MC quantities as done in the data. All the parameters in the MC are set by
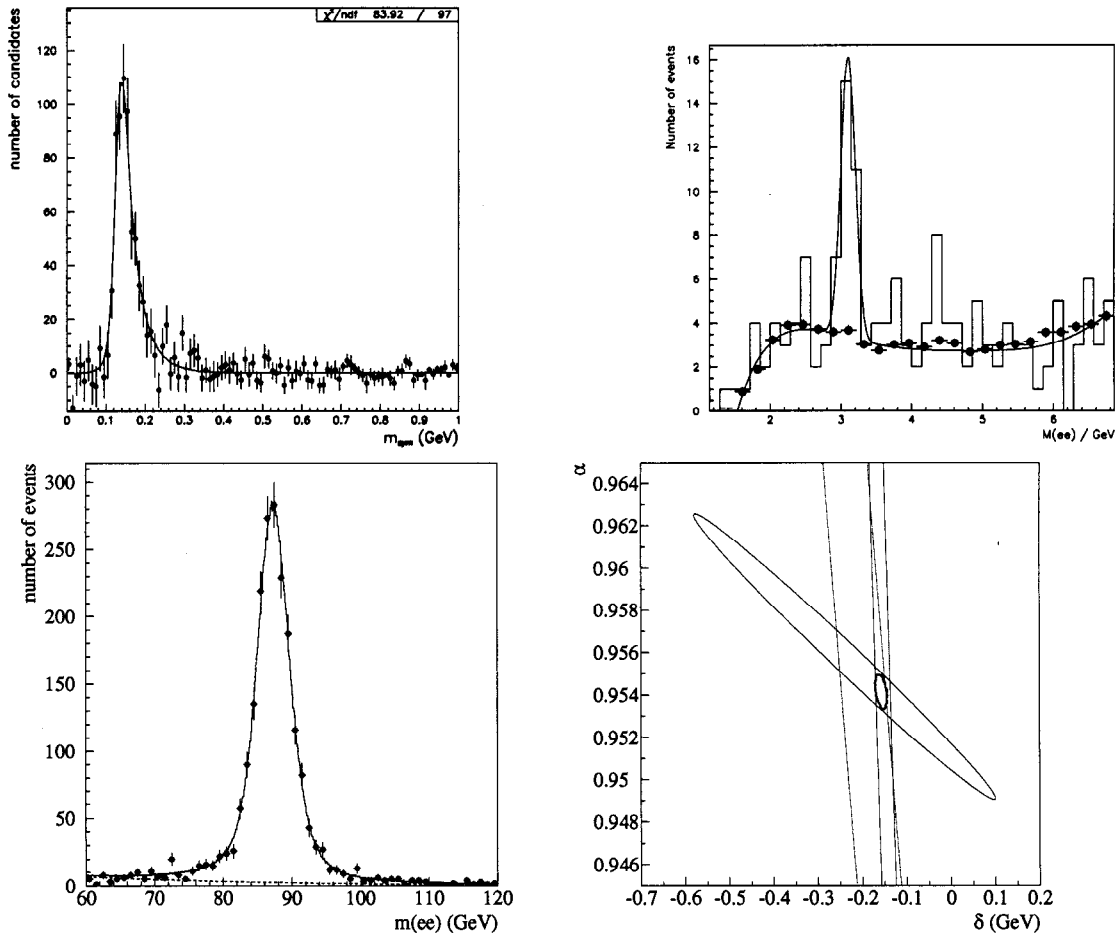
FIG. 4. The invariant mass distributions are shown for (a) $\pi^0 \rightarrow \gamma\gamma \rightarrow e^+e^-e^+e^-$ events (points), (b) $J/\psi \rightarrow ee$ events (points), and (c) $Z \rightarrow ee$ events (points), compared to Monte Carlo simulations (line). (d) Constraints on α and δ from $Z \rightarrow ee$ decays (large ellipse), $J/\psi \rightarrow ee$ decays (wide band), $\pi^0 \rightarrow \gamma\gamma \rightarrow e^+e^-e^+e^-$ decays (narrow band), and for all three combined (small ellipse).

Z data and other data samples. Below is a discussion of the determination of the parameters in the W Monte Carlo. The Z data are treated in an analagous fashion. Systematic errors are set using large statistics samples of MC data and varying the parameter within its errors and are discussed throughout.

The W production is modelled by the double differential cross section in $p_T(W)$ and rapidity, y, calculated at next-to-leading order by Ladinsky and Yuan [12] and using the MRSA [13] pdf. The W resonance is generated by a relativistic Breit-Wigner, incorporating the mass dependence of the parton momentum distribution:

FIG. 5. (a) Comparison of the $u_\parallel$ distribution from $W \to e\nu$ events (points) and the MC simulation (histogram); (b) C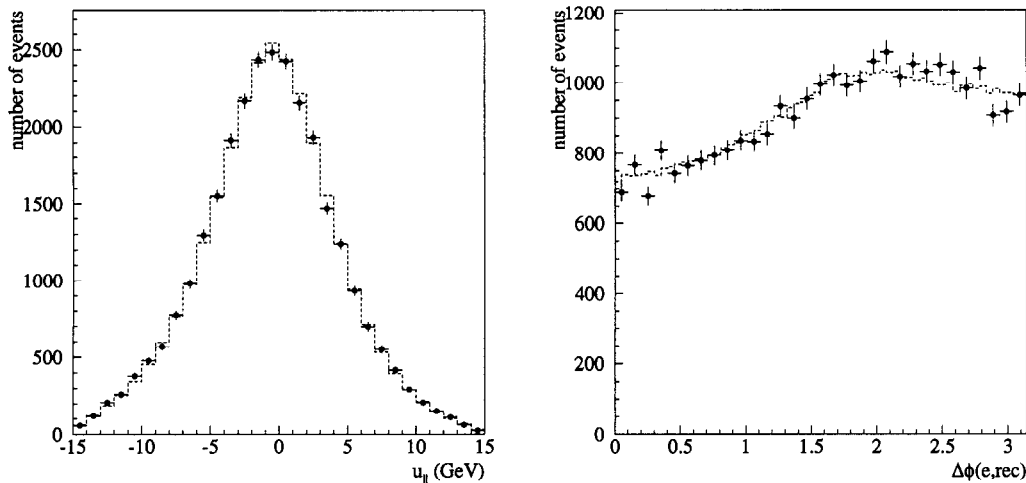omparison of the angle between the recoil and the electron in the transverse plane from $W \to e\nu$ events (points) and the MC simulation (histogram).

$$\frac{d\sigma}{dm} \sim \frac{e^{-\beta \cdot m}}{m} \cdot \frac{m^2}{(m^2 - M_W^2)^2 + \frac{m^4 \Gamma^2}{M_W^2}}.$$

The angular decay products are generated at $\mathcal{O}(\alpha_s)$, allowing $p_T(W) > 0$, in the W rest frame. This angular decay is of the form [14]

$$\frac{d\sigma}{d\cos\theta} \sim \left(1 + \alpha_1 \cos\theta + \alpha_2 \cos^2\theta\right)$$

where $\alpha_{1,2} = \alpha_{1,2}(p_T(W))$ [14]. Radiative decays ($W \to e\nu\gamma$) are generated according to Berends and Kleiss [15]. Events in which $W \to \tau\nu \to e\nu\bar\nu\nu$ are indistinguishable from $W \to e\nu$ decays and are therefore modelled in the simulation, including the polarization of the τ in the decay angular distribution. The decay products are then boosted to the laboratory frame. At this point, the values of $p_T(e)$ and $p_T(W)$ have been generated and $p_T(\nu)$ is calculated. The effects of the detector and underlying event are now modelled.

The EM (electron) calorimeter energy scale of the calorimeter was determined using $J/\psi \to ee$, $\pi^0 \to \gamma\gamma \to e^+e^-e^+e^-$, and $Z \to ee$ events. From test beam studies, it was determined that a linear relationship between the true and measured energies could be assumed: $E_{\text{meas}} = \alpha E_{\text{true}} + \delta$. This gives a relation $M_{meas} = \alpha M_{true} + \delta f$ between the measured and true mass values, keeping terms to first order in δ only. The variable $f = \frac{2(E_1 + E_2)}{M} \sin^2 \frac{\gamma}{2}$ depends on the event decay topology. Since the ratio of M_W to M_Z is actually measured, one finds

$$\left(\frac{M_W}{M_Z}\right)^{meas} = \left(\frac{M_W}{M_Z}\right)^{true} \left[1 + \frac{f\delta}{\alpha} \cdot \frac{(M_Z - M_W)}{M_W M_Z}\right].$$

12
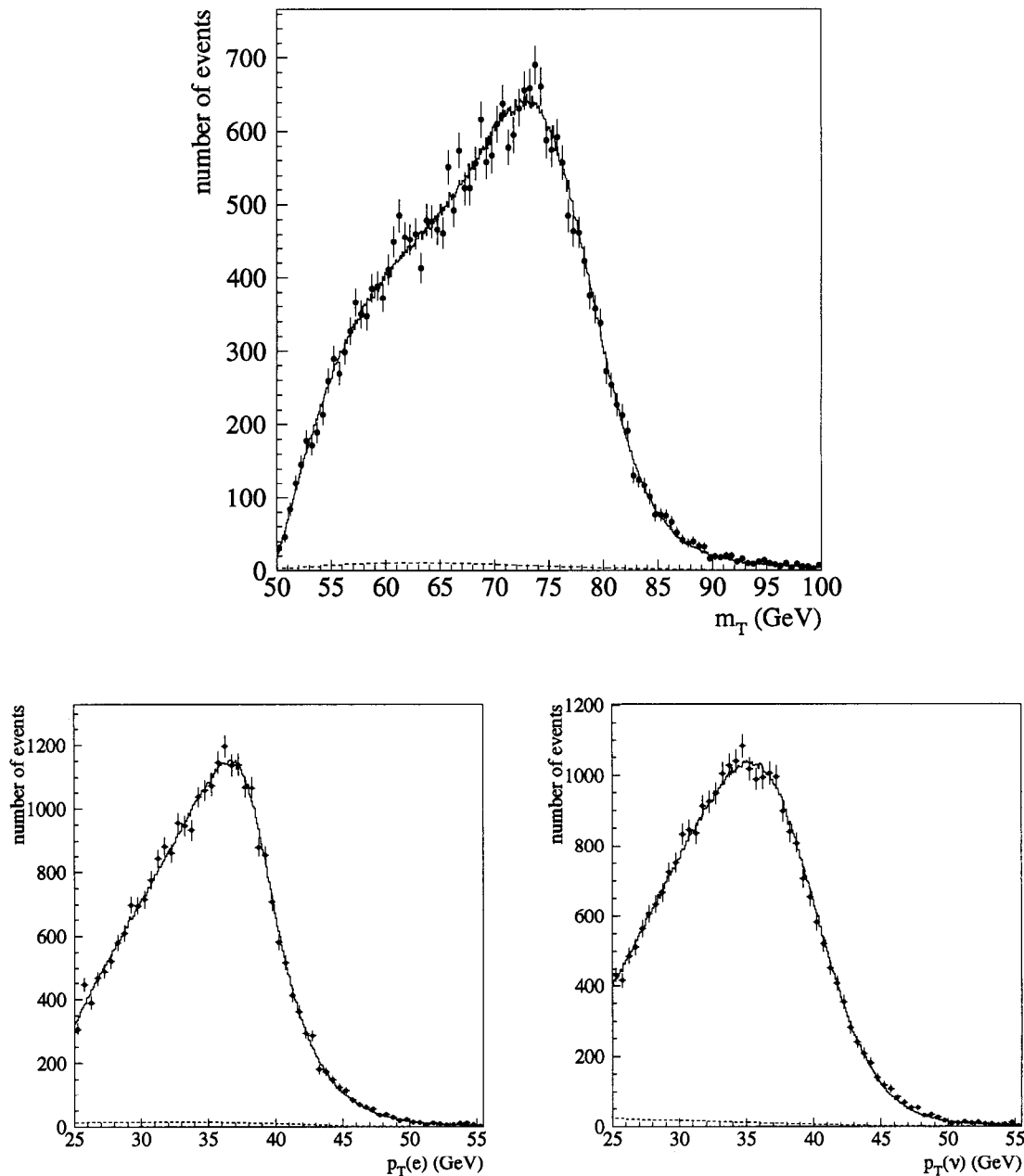
FIG. 6. (a) The transverse mass distribution, (b) the electron transverse momentum distribution, and (c) the neutrino transverse momentum distribution are shown for W events (points). The best fits of the MC simulation (histograms) are also shown.

We note that to first order the measured ratio is insensitive to the EM energy scale, if δ is small, and that the error on the measured ratio due to the uncertainty in δ is suppressed.

Figure 4 shows the mass spectra for the $\pi^0, J/\psi$ and Z data samples. The allowed ranges for α and δ are shown in Fig. 4d for each data sample. The overlap region is the 1σ contour

13

FIG. 7. The DØ determination of the mass of the top quark is shown versus the measured W mass. The SM prediction (see text) for various assumptions of the Higgs boson mass is indicated by the bands.

from all three data samples. The scale α is fixed by the Z data. The value of δ is constrained by the J/ψ and π^0 data, essentially independent of α. Allowing a quadratic term in the energy response, to account for nonlinear responses at low energies 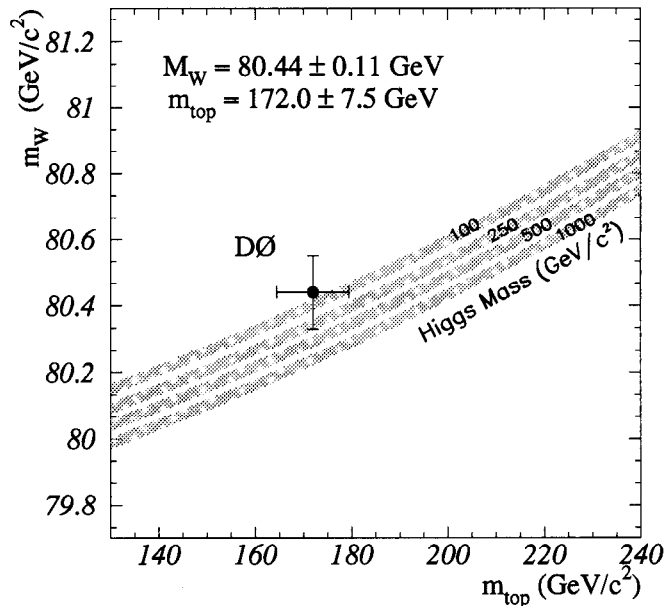as measured at the test beam, leads to the systematic error on δ. The allowed values determined for α and δ are $\alpha = 0.95329 \pm 0.00077$ and $\delta = -0.160 \pm 0.016(stat.)\,^{+.060}_{-.210}(syst.)$ GeV. The error in the EM energy scale introduces an uncertainty in M_W of ± 65 MeV/c^2 and is dominated by the statistical error in determining the Z mass.

The EM energy resolution is parameterized as $\sigma/E = \sqrt{C^2 + (S/\sqrt{E_T})^2 + (N/E)^2}$ for the central calorimeter. Test beam data are used to set the sampling term, $S = 0.13$ (GeV$^{1/2}$), and the noise term, $N = 0.4$ GeV. By constraining the width of the Z invariant mass distribution in the MC to that from the data, the constant term is set to $C = \left(1.15 \,^{+0.27}_{-0.36}\right)$. The uncertainty in the energy resolution leads to an uncertainty of ± 23 MeV/c^2 in M_W.

The hadronic (recoil) energy scale of the calorimeter is determined relative to the EM energy scale by using Z events and measuring the transverse momenta of the Z from both the recoil or the two electrons. The p_T−balance is constructed:

$$p_T-\text{balance} \equiv [\vec{p}_T(ee) + \vec{p}_T(rec)] \cdot \hat{\eta}$$

where $\hat{\eta}$ is defined as the bisector of the two electrons. From studies using HERWIG [16] and GEANT [17], it was determined that the recoil response could be written as a function

14

of the EM response: $p_T(rec) = \mathcal{R}_{rec} p_T(ee)$ with $\mathcal{R}_{rec} = \alpha_{rec} + \beta_{rec}\log p_T(W)$. To ensure an equivalent event topology, Z events in which one electron is in the forward region are included in this study. Comparing data to MC in a plot of p_T−balance versus $\vec{p}_T(ee) \cdot \hat{\eta}$, the recoil response parameters are determined to be $\alpha_{rec} = 0.69 \pm 0.06$ and $\beta_{rec} = 0.04 \pm 0.02$. The uncertainty in the recoil scale leads to an uncertainty of ± 23 MeV/c^2 in M_W.

The recoil (hadronic) energy resolution is determined by modelling both components of the recoil to the W: $\vec{p}_T(rec)^{meas} = \mathcal{R}_{rec}\vec{p}_T(rec) + \alpha_{mb} \cdot \vec{U}_{mb}(tot) - U(\hat{e})$. The first component is the "hard" component due to the initial p_T of the boson. It is smeared using a Gaussian of width $\sigma_{rec} = s_{rec}\sqrt{p_T(rec)}$. The second component is the "soft" component due to the underlying event and is modelled by a minimum-bias event obtained from the data. In selecting the minimum-bias events to use, the luminosity distribution of the W event sample is modelled. The quantity $\vec{U}_{mb}$ is the total $\vec{E}_T$ of minimum-bias event and α_{mb} is a scale factor. The amount of underlying event in the electron direction, $U(\hat{e})$, is subtracted from the recoil and added onto the electron momentum. Using the width of the p_T−balance distribution (to which the energy calibration has been applied), the values of s_{rec} and α_{mb} are constrained. The measured values are $s_{rec} = 0.49 \pm 0.14$ and $\alpha_{mb} = 1.03 \pm 0.03$ and their errors and lead to an uncertainty of of ± 33 MeV/c^2 in M_W.

Selection biases due to radiative decays and the amount of recoil energy in the electron direction and trigger efficiences are modelled in the MC simulation. The uncertainty in M_W due to the modelling of these efficiencies and biases is negligible in the fit to the $M_T(W)$ spectrum.

Backgrounds to the W event sample are included in the fitting procedure by including the shape and fraction of background events. The largest source of background in the W sample is due to QCD multijet production in which there is a jet is mis-identified as an electron and $\not{E}_T$ due to energy fluctuations. This background contributes $1.4 \pm 0.2\%$ to the W sample. The other background considered is $Z \rightarrow ee$ events where one electron is not identified. This background contributes $0.33 \pm 0.06\%$ to the W sample. The uncertainty in size and shape of the backgrounds gives an uncertainty in M_W of ± 12 MeV/c^2. All other sources of background are negligible.

The last systematic error to consider is that due to the modelling of the W production. This uncertainty is due to the correlated uncertainties in the $p_T(W)$ spectrum and the pdf's. There are three phenomenological parameters in the production model calculation (g_1, g_2, g_3) [12] and the largest sensitivity of the p_T spectrum is to the g_2 parameter. To constrain the production model, the g_1 and g_3 parameters are fixed to their nominal values and the value of g_2 is constrained by the $p_T(Z)$ distribution from the data. Then the dependence of M_W on the pdf used in the theoretical calculation is measured from the difference in M_W from the nominal pdf (MRSA) as seen in Table IV. For each pdf, the theoretical calculation uses the value of g_2 constrained by the data for that case. The uncertainties on the measured M_W due to the value of g_2 and the pdf used are ± 5 MeV/c^2 and ± 21 MeV/c^2, respectively. Errors on M_W are also ascribed to uncertainties in the value of $\Gamma_W \rightarrow \pm 9$ MeV, the parton luminosity parameter $\rightarrow \pm 10$ MeV, and the modelling of radiative decays $\rightarrow \pm 20$ MeV. The total uncertainty on M_W due to the production model is $\sigma(M_W) = \pm 34$ MeV.

A measure of how accurately the MC describes the data is shown in Fig. 5. The quantity $u_{\parallel} = \vec{p}_T(rec) \cdot \hat{e}$, which is the hadronic energy in electron direction, is shown in Fig. 5a.

pdf	constrained g_2	ΔM_W MeV
MRSA	0.59	-
MRSD-	0.61	+20
CTEQ3M	0.54	+5
CTEQ2M	0.61	-21

TABLE IV. The variation of the measured W mass when using different pdf's in the production model. Each theoretical calculation uses the constrained value of g_2 for that pdf.

A bias in $u_{\parallel}$ directly affects the $M_T(W)$ spectrum and it is also very sensitive to the recoil resolution. Another sensitive quantity is the difference in the azimuthal angle, $\Delta\phi$, between the electron and the recoil and is shown in Fig. 5b. Excellent agreement between the data and MC simulation is obtained.

Source	$\sigma_{M(W)}$ in MeV/c^2
Statistical (W events)	69
Statistical (Z events)	65
Non-Uniform energy response (η)	10
Electron Angle Calibration	28
Electron Energy Resolution	23
Electron Energy Linearity	20
Electron Underlying Event	16
Hadronic Energy Scale	20
Hadronic Resolution	33
$P_T(W)$ Spectrum	5
pdf	21
parton luminosity	10
W Width	9
Radiative Decays	20
QCD background	11
Z background	5
Systematic Total	70
Total	118

TABLE V. Summary of errors on the W mass measurement.

The $M_T(W)$ distribution from the data is shown in Fig. 6a together with the distribution from the best fit value of M_W from the Monte Carlo simulation. The data are fit over a region 60 to 90 GeV/c^2 and the preliminary value of the W mass determined is $M_W = 80.450 \pm$

$0.070(stat.) \pm 0.065(scale) \pm 0.070(syst.)$ GeV/c^2, giving a total error of ± 118 MeV/c^2. The errors on the W mass are detailed in Table V.

As consistency checks, the $p_T(e)$ and $p_T(\nu)$ spectra are also fit to determine M_W as shown in Figs. 6b and 6c. The fit to the $p_T(e)$ spectrum gives $M_W = 80.49 \pm 0.14$ GeV/c^2 and the $p_T(\nu)$ fit gives $M_W = 80.42 \pm 0.18(stat.)$ GeV/c^2 with the fitting region from 30 to 50 GeV/c in both cases.

In summary, the measured W masses from the DØ data sample of $W \rightarrow e\nu$ decays with the e in the central η region are $M_W = 80.35 \pm 0.27$ GeV/c^2 (run 1A) and $M_W = 80.45 \pm 0.12$ GeV/c^2 (run 1B, preliminary). Combining these results and taking into account the correlated errors gives a DØ combined value of $M_W = 80.44 \pm 0.11$ GeV/c^2.

Combining the new DØ result with other measurements [18,19] from hadron collider experiments gives a new preliminary hadron collider average of $M_W = 80.41 \pm 0.09$ GeV/c^2.

The constraints placed on the Higgs mass can be seen in Fig. 7, which shows the measured values of M_W versus m_{top} [20] compared to the Standard Model prediction [21] for different values of the M_H in the $m_{top} - M_W$ plane.

V. CONCLUSIONS

In conclusion, DØ has collected ≈ 100pb^{-1} of data from run 1 of the Tevatron and preliminary results on W boson properties are found to be in agreement with the Standard Model. The W and Z cross sections are measured in the e, μ, τ decay modes. The W width is measured to be $\Gamma_W = 2.159 \pm 0.092$ GeV. We confirm $e - \tau$ universality in W decays with the measurement $g_\tau^W/g_e^W = 1.004 \pm 0.032$. The run 1 combined DØ W mass, $M_W = 80.44 \pm 0.11$ GeV/c^2, is currently the most accurate direct measurement.

ACKNOWLEDGEMENTS

REFERENCES

* Visitor from IHEP, Beijing, China.

† Visitor from Universidad San Francisco de Quito, Quito, Ecuador.

[1] S. Weinberg, Phys. Rev. Lett. **19**, 1264 (1967);
A. Salam, in *Elementary Particle Theory*, ed. by N. Svartholm (Almquist and Wiksell, Sweden, 1968), p. 367;
S.L. Glashow, J. Illiopoulos and L. Maiani, Phys. Rev. D **2**, 1285 (1970).

[2] S. Abachi *et al.*, (DØ Collaboration), Nucl. Instrum. Methods **A338**, 185 (1994).

[3] S. Abachi *et al.*, (DØ Collaboration), Phys. Rev. Lett. **75**, 1456 (1995) and references therein.

[4] F. Abe *et al.*, (CDF Collaboration), Phys. Rev. Lett **76**, 3070 (1996).

[5] H. Hamberg, W.L. van Neerven and T. Matsuura, Nucl. Phys. B **359**, 343 (1991); W.L. van Neerven and E.B. Zijlstra, Nucl. Phys. B bf 382, 11 91992).

[6] H.L. Lai *et al.*, Phys. Rev. **D51**, 4763 (1995).

[7] Particle Data Group, L. Montanet *et al.*, Phys. Rev. **D50** 1173 (1994).

[8] We use ref. [5] with the CTEQ2M pdf, $M_W = 80.23 \pm 0.18$ GeV, $M_Z = 91.19$ GeV and $\sin^2 \theta_W = 0.2259$.

[9] J.L. Rosner, M.P. Worah and T. Takeuchi, Phys. Rev. **D49**, 1363 (1994) with $M_W = 80.23 \pm 0.18$ GeV.

[10] S. Abachi *et al.*, (DØ Collaboration), Phys. Rev. Lett. **77**, 3309 (1996).

[11] CERN-PPE/95-172, LEP Electroweak Working Group, 1995.

[12] G. Ladinsky, C.P. Yuan, Phys. Rev. D**50**, 4239 (1994).

[13] A.D. Martin, R.G. Roberts and W.J. Stirling, Phys. Rev. D**50**, 6734 (1994) and A.D. Martin, R.G. Roberts and W.J. Stirling, Phys. Rev. D**51**, 4756 (1995).

[14] E. Mirkes, Nucl. Phys. B **387**, (1992) 3.

[15] F. A. Berends and R. Kleiss, Z. Phys. C**27**, 365 (1985).

[16] G. Marchesini and B.R. Webber, Nucl. Phys. B **310** (1988) 461.

[17] F. Carminati *et al.*, GEANT User's Guide, CERN Program Library (Dec. 1991).

[18] J. Alitti *et al.*, (UA2 Collaboration), Phys. Lett., B**276**, 354 (1992).

[19] F. Abe *et al.*, (CDF Collaboration), Phys. Rev. Lett. **65**, 2243 (1990); Phys. Rev. D**43**, 2070 (1991); Phys. Rev. Lett. **75**, 11 (1995); Phys. Rev. D**52**, 4784 (1995).

[20] S. Abachi *et al.*, (DØ Collaboration), Phys. Rev. Lett. **74**, 2632 (1995). See also "Direct Measurement of the Top Quark Mass", S. Abachi *et al.*, (the DØ Collaboration), FERMILAB-PUB-97/059-E, to be published in Phys. Rev. Lett. and "Measurement of the Top Quark Mass Using Dilepton Events", B. Abbott *et al.*, (DØ Collaboration), FERMILAB-PUB-97/172-E, Submitted to Phys. Rev. Lett.

[21] ZFITTER: D. Bardin et al., Z. Phys. C**44**, 493 (1989); Comp. Phys. Comm. **59**, 303 (1990); Nucl. Phys. B**351**, 1 (1991); Phys. Lett. B**255**, 290 (1991); and CERN-TH 6443/92 (May 1992).